scientific reports

OPEN

Design and numerical evaluation of a high sensitivity plasmonic biosensor based on MISM nanoring for versatile virus detection

Ali Khodaie, Yousef Rafighirani, Hamid Heidarzadeh✉ & Javad Javidan

Recent advancements in nanotechnology have positioned plasmonic optical sensors as powerful tools for biosensing applications. These sensors utilize the interaction of electromagnetic waves with metallic nanostructures to enable rapid, label-free detection of biological analytes. In this study, we propose and optimize a plasmonic optical biosensor based on nanohole arrays and metal–insulator–semiconductor–metal (MISM) nanorings for detecting various viruses. The sensor structure incorporates gold and silver layers on a silver substrate, with the nanohole and nanoring elements engineered to enhance sensitivity to refractive index variations in the surrounding medium. The finite-difference time-domain (FDTD) method evaluates the sensor's performance, which numerically solves Maxwell's equations for frequency-dependent optical behavior. Simulation results demonstrate the sensor's capability to detect minute refractive index changes induced by viruses such as HSV, HIV-1, Influenza A, and M13 bacteriophage. The design achieves a high sensitivity of 811 nm/RIU, attributed to Fano resonance effects and optimized geometrical parameters. Furthermore, the sensor exhibits a figure of merit (FOM) of 3.38 RIU^{-1} and a limit of detection (LoD) of 0.268 RIU, outperforming many previously reported plasmonic biosensors. These findings underscore the potential of nanohole–MISM nanoring-based plasmonic sensors for rapid, label-free, and highly sensitive virus detection. With further development in structural design and fabrication techniques, this platform could be widely applicable in medical diagnostics and point-of-care biosensing.

Keywords Optical biosensor, Sensitivity, Various viruses, Nanoholes, Metal-insulated-semiconductor-metal (MISM) nanorings

With the advancement of nanotechnology and the increasing need for more sensitive and precise methods for virus detection, plasmonic optical sensors have emerged as innovative and efficient tools in biosensing. These sensors, which operate based on the interaction of electromagnetic waves with metallic nanostructures, enable rapid and indirect detection of biological compounds. A key advantage of these sensors is their high sensitivity to minute refractive index changes in the environment surrounding the metallic nanostructures, allowing them to identify various viral species[1]. A novel structure in the field of plasmonic optical sensors is the use of metal-insulator-metal (MIM) nanostructures, which offer superior performance compared to other plasmonic structures due to their unique characteristics. These structures, typically made from metals such as gold and silver, are considered suitable for designing advanced biosensors due to their chemical stability and favorable optical properties. The integration of nanoholes and nano-rings in MIM structures enhances the interaction of light with biological samples, thereby improving the sensitivity and accuracy of the sensor[2]. In the design of plasmonic optical circuits, two types of surface plasmon polariton (SPP) waveguides are employed: metal-insulator-metal and insulator-metal-insulator (IMI)[3]. Sensors based on MIM waveguides offer several advantages over IMI, including reduced propagation losses, improved plasmonic mode confinement, enhanced tunability, and better compatibility with fabrication processes[4]. Particularly, the tunability of Fano resonance plays a crucial role in enhancing the performance of these sensors, as it allows for independent adjustment of resonant features[5]. To analyze and solve time-dependent electromagnetic problems, the finite-difference time-domain (FDTD) method is utilized. In this method, Maxwell's equations are numerically discretized and solved on a computational grid. Fano resonance, resulting from the interaction of bright and dark modes in the radiative spectrum, is considered

Department of Electrical and Computer Engineering, University of Mohaghegh Ardabili, Ardabil, Iran. ✉email: heidarzadeh@uma.ac.ir

an ideal choice for sensing applications due to its asymmetric and sharp transmission spectrum. Compared to Lorentzian resonance, Fano resonance exhibits higher sensitivity to changes in geometric and environmental parameters, thereby providing greater accuracy in detecting biological changes[6]. Recent studies have shown that Fano resonance-based designs, such as systems incorporating split-ring resonators or specific cavity structures, can achieve high sensitivity for detecting biological compounds[7]. Given the importance of high accuracy and sensitivity in viral disease detection, the design and optimization of plasmonic optical sensors using advanced nanostructures have become a key focus in the fields of bioengineering and photonics. This paper presents the design and numerical analysis of a plasmonic optical sensor based on MIM nanoholes and nano-rings, optimized for the detection of various viruses. The study also evaluates how structural parameters affect sensor performance, comparing results with prior work on MIM nanostructures[8].

Among the innovative structures, metal-insulator-semiconductor-metal (MISM) configurations have attracted attention due to their superior performance compared to traditional plasmonic designs. MISM structures, which are typically fabricated using gold and silver, are of interest for advanced biosensors due to their chemical stability and favorable optical properties. The incorporation of these materials enhances light-matter interaction and improves sensitivity and accuracy[2]. Fano resonance, which arises from the interaction of light and dark states, is particularly useful for sensing applications due to its sharp and asymmetric transmission spectrum. Compared to Lorentz resonance, Fano resonance exhibits higher sensitivity to geometric and environmental variations, thereby increasing the detection accuracy[8]. Recent studies have highlighted the potential of Fano resonance-based designs, such as split-ring resonators or specific cavity structures, to achieve high sensitivity in the detection of biological compounds[9]. Given the critical need for accurate and sensitive tools in virus detection, optimization of plasmonic optical sensors using advanced nanostructures has become a focal point in bioengineering and photonics research. This study presents the design and numerical analysis of a plasmonic optical biosensor based on MISM nanoparticles optimized for the detection of various viruses. The influence of structural parameters on the sensor performance is fully evaluated, and the results are compared with previous studies on MIM nanostructures[7]. This research highlights the potential of MISM-based plasmonic optical sensors for rapid and accurate virus detection, overcoming limitations observed in previous designs. Further advances in fabrication and design could expand their applications in medical diagnostics and biosensing.

Structure and method

The emergence of metamaterials has paved the way for the development of metal-insulator-semiconductor-metal nanoring structures. These structures, composed of subwavelength metallic elements, exhibit a robust electromagnetic response. Metamaterials possess unique properties, such as electrical conductivity and negative magnetic permeability, making them highly suitable for designing MISM nano-rings. Gold and silver have been recognized as the most significant for constructing these structures among the various available metamaterials. This study uses gold and silver to fabricate a plasmonic optical biosensor incorporating nanoholes and MISM nano-rings. The sensor is built on a silver substrate, and the optical properties of gold and silver are derived from the data provided by Palik[10]. The integration of nanoholes and MISM nanoring technology into optical sensors enables a simple structure and convenient design. These sensors offer superior performance compared to other plasmonic sensors, motivating researchers to explore their potential further. This section describes the structure and dimensional parameters of the plasmonic optical biosensor, which is based on nanoholes and MISM nano-rings. Typically, the design of MISM nano-rings consists of single or multiple metallic rings, available in different geometries such as circular or square shapes. Gold and silver are the primary materials used for fabricating these nano-rings. When exposed to a time-varying magnetic field, an annular electric current is induced within the metal nano-rings, generating a magnetic dipole moment perpendicular to the rings. As illustrated in Fig. 1, the designed structure consists of a square nanocavity with side length d and depth h_r within a silver cube of length L. Inside this nanocavity, three nested nano-rings made of silver, silicon, and silver are arranged with inner and outer radii R_{in} and R_{out}, respectively. A small cylindrical nanoparticle with a very small radius is placed at the center of these nano-rings. The thickness of the nano-rings is denoted as h_r. Additionally, to enhance the performance of the sensor, a substrate layer with thickness h_{sub} is positioned beneath the nanocavity. The materials and dimensional parameters of the structure will be analyzed to optimize the sensor's performance, and Table 1 presents the final optimized dimensions.

Plasmonic losses and defects resulting from manufacturing tolerances significantly affect the performance of plasmonic systems. Due to their intrinsic properties, plasmonic metals experience energy losses primarily due to ohmic heating, which reduces the strength of localized electric fields and impacts their application in biosensing. The extent of these losses depends on the chosen material. Additionally, manufacturing defects pose considerable challenges, as imperfections in production can increase scattering losses and reduce the system's efficiency. For instance, surface roughness in metallic structures can intensify scattering during state transitions, leading to greater energy dissipation. Furthermore, these defects can cause misalignment and dimensional inconsistencies in plasmonic structures, creating discrepancies between experimental results and theoretical predictions. By carefully optimizing geometric parameters, selecting suitable materials, and improving fabrication techniques, the efficiency and functionality of plasmonic devices can be enhanced, leading to new technological applications[11]. A common limitation of plasmonic biosensors, as mentioned in previous studies, is the lack of versatility in detecting a wide range of viruses with distinct refractive indices. Previous designs often focused on specific analytes or lacked the structural optimization required for high sensitivity and practical stability under environmental conditions (e.g., temperature, angle, polarization). This creates a gap in the development of highly sensitive and robust plasmonic sensors capable of rapid and accurate detection of multiple viruses for real-world diagnostics.

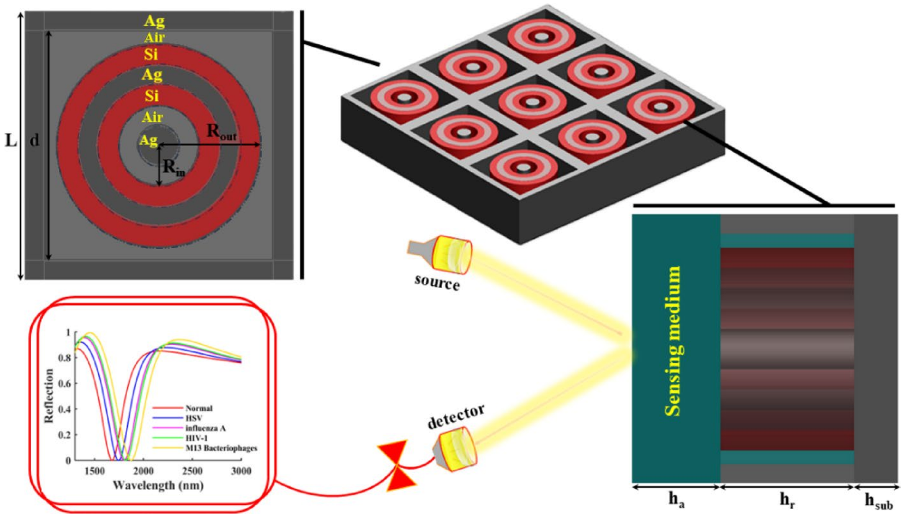

Fig. 1. Schematic of the designed structure as a nanohole–metal–insulator–semiconductor–metal (MISM) Nanoring-Based Plasmonic Biosensor.

Parameter	Symbol	Value (nm)
Substrate outer length	L	200
Substrate inner length	d	170
The outer radius of the ring	R_{out}	76
The inner radius of the ring	R_{in}	35
Substrate thickness	h_{sub}	50
Rings thickness	h_r	150
Analyte thickness	h_a	100

Table 1. Dimensional parameters of the sensor after optimization.

n	Virus
1.33	Normal
1.41	HSV
1.48	Influenza A
1.50	HIV-1
1.57	M13 bacteriophages

Table 2. Refractive index of various viruses for the detection in this study.

The implementation of MISM nanoring configurations, which are highly adaptable systems for detecting various medical samples, including viruses, in laboratory environments, begins with their design and fabrication. To manufacture these structures, advanced nanofabrication techniques such as electron beam lithography (EBL), focused ion beam lithography (FBL), and nanoimprint lithography are employed[12]. Furthermore, MISM nanoring structures are integrated with microfluidic systems to analyze the intricate permeability properties of liquid medical samples. When different biological samples interact with the MISM nanoring system, they alter the optical properties of the sensing environment, causing a shift in resonance frequency. These shifts are then measured to evaluate the changes in the sample's characteristics[4]. The used refractive index for various viruses is presented in Table 2.

The proposed configuration is analyzed using the finite difference time domain (FDTD) numerical method, incorporating the Yee algorithm to solve Maxwell's governing equations. To achieve this, the widely used commercial software, Lumerical FDTD Analyzer, is employed within the fields of optics, photonics, and nanoelectronics. In the FDTD method, the mesh is set to auto-non-uniform mode, and the Conformal0 mode is applied to refine the mesh. The mesh accuracy is set to '8'. To ensure the simulation converges efficiently while maintaining precision, a separate mesh with element sizes of dx = dy = dz = 4 nm is specifically used for the structure-sensitive regions of the MIM nano-rings. The background refractive index is assumed to be 1, corresponding to air. Additionally, the simulation runs for 1000 femtoseconds at a temperature of 300 K, using the Field Time monitor. Perfectly Matched Layer (PML) boundary conditions are applied along the z-axis, while periodic boundary conditions are used in the x and y directions. A plane wave source emits light with wavelengths ranging from 1300 to 3500 nm. The reflection spectrum is measured using the Frequency-Domain Field and Power Monitor, while the electromagnetic field distribution is visualized using the Frequency-Domain Field Profile Monitor.

To assess sensor performance metrics, such as sensitivity and figure of merit (FOM), a target analyte layer can be placed on the SRR structure. By varying the refractive index of the analyte (Δn_s), a shift in the resonance wavelength ($\Delta\lambda_0$) within the reflection spectrum is observed. Sensor sensitivity is mathematically expressed as follows[1]:

$$S=\frac{\Delta\lambda_0}{\Delta n_s} \tag{1}$$

The FOM serves as a key performance indicator for evaluating the overall effectiveness of an optical sensor. This metric consolidates multiple parameters, such as sensitivity and response time, into a single value, facilitating comparative analysis across different sensor designs. The FOM of a sensor is mathematically defined using the following equation[13]:

$$\mathrm{FOM}=\frac{S}{\mathrm{FWHM}} \tag{2}$$

In this context, FWHM (Full Width at Half Maximum) plays a crucial role in characterizing the quality of resonances within the reflection spectrum. This parameter provides insight into the sensor's performance and sensitivity, with a narrower FWHM indicating improved resolution for detecting biological samples.

Also, the smallest measurable quantity the sensor can detect, known as the Limit of Detection (LoD), is defined as follows[8]:

$$\mathrm{LoD}=\left(\frac{\Delta\ \mathrm{n_s}}{1.5}\right)\times\left(\frac{\mathrm{FWHM}}{\Delta\ \lambda_0}\right)^{1.25} \tag{3}$$

Furthermore, the proposed biosensor is evaluated using several metrics, detection accuracy (DA), signal-to-noise ratio (SNR), and Severity Rating (SR), which are defined by the following equations[14]:

$$\mathrm{DA}=\frac{1}{\mathrm{FWHM}} \tag{4}$$

$$\mathrm{SNR}=\frac{\Delta\ \lambda_0}{\mathrm{FWHM}} \tag{5}$$

$$\mathrm{SR}=\mathrm{S.LoD} \tag{6}$$

Results and discussion

This section presents the results of simulations conducted for the plasmonic optical biosensor based on nanoholes and metal-insulator-semiconductor-metal (MISM) nanorings. The primary objective is to evaluate the sensor's performance under various conditions and analyze the impact of structural and environmental parameters on its sensitivity and accuracy. For this purpose, the finite-difference time-domain (FDTD) method was employed, enabling precise analysis of the structure's electromagnetic behavior[15]. The results demonstrate that the proposed design can detect minute changes in the refractive index of the surrounding environment, caused by the presence of various viruses such as HSV, HIV-1, influenza A, and M13 bacteriophages. Additionally, the effects of various parameters, including substrate thickness, nano ring dimensions, and nanorings thickness, were thoroughly investigated. These analyses have significantly contributed to optimizing the sensor's structure and enhancing its performance. In the following sections, the results related to each parameter are discussed in detail, and their impact on the reflectance spectrum and sensor sensitivity is analyzed. These investigations not only highlight the superior performance of the proposed sensor but also provide insights for further improvements in the future. Figure 2(a) shows the reflectance spectra of the sensor for substrates made of gold and silver. The results indicate that the silver substrate exhibits a stronger plasmonic response compared to the gold substrate, leading to sharper resonance peaks and higher sensitivity. This phenomenon is attributed to silver's superior optical properties and lower ohmic losses compared to gold. Due to its lower refractive index and greater ability to concentrate electromagnetic fields, silver is considered an ideal material for the substrate. Figure 2(b) compares the reflectance spectra of the sensor for nano-rings made of gold and silver. The results demonstrate that silver nano-rings provide a stronger plasmonic response compared to gold nano-rings. This is due to silver's favorable optical properties, including lower light absorption and reduced energy losses. Silver nano-rings produce narrower and more intense resonance peaks, significantly enhancing the sensor's sensitivity. Therefore, silver is selected as the superior material for fabricating nano-rings in this sensor.

In the optimization of the sensor's structural dimensions (as illustrated in Fig. 3), the Particle Swarm Optimization (PSO) algorithm was employed to achieve the most efficient design parameters. PSO is a computational optimization technique inspired by the social behavior of biological systems, such as bird flocking or fish schooling[16]. In this algorithm, a population of candidate solutions, referred to as "particles," moves through the search space to find the optimal solution. Each particle adjusts its position based on its own experience (local

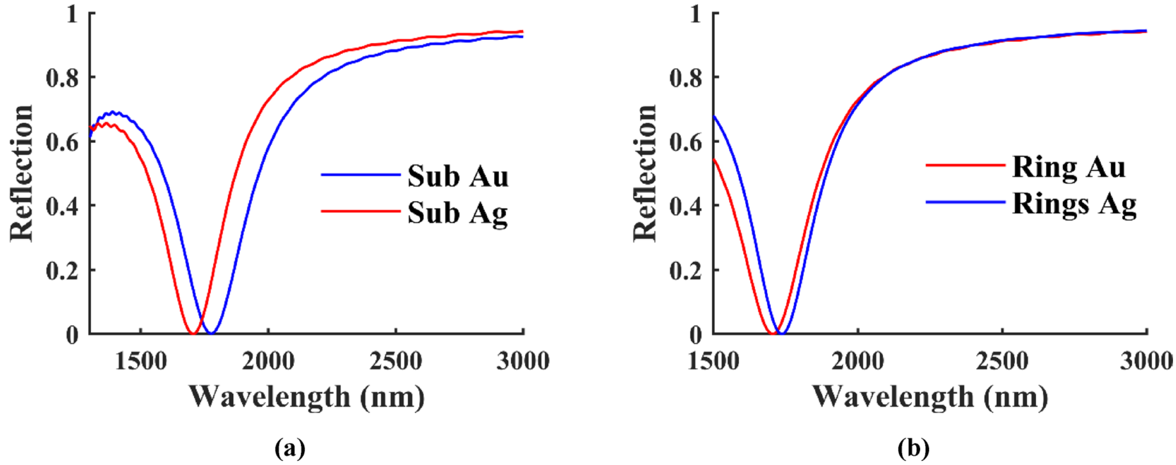

Fig. 2. Reflectance spectra of the proposed structure versus gold (Au) and silver (Ag) materials for **(a)** substrate and **(b)** nano-rings.

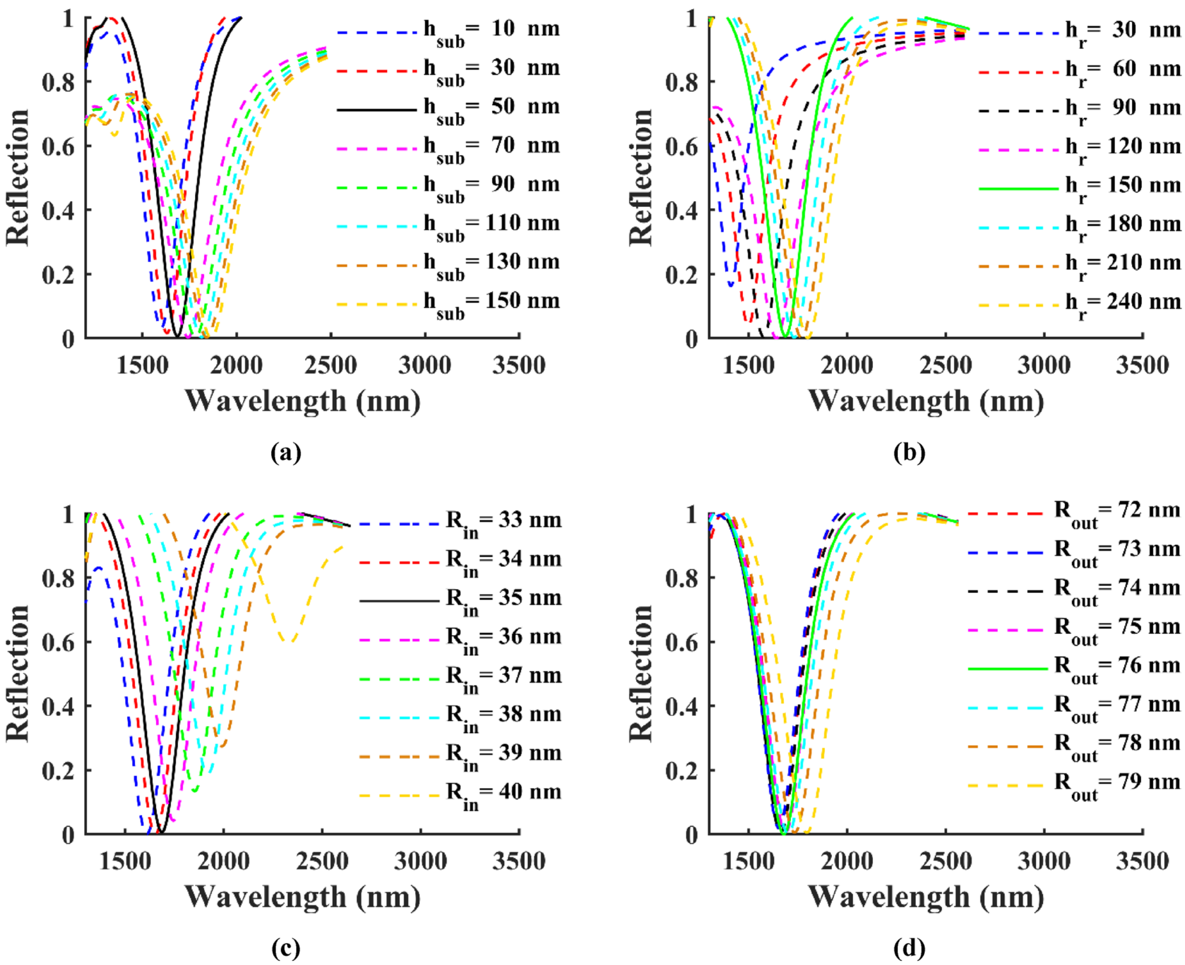

Fig. 3. Reflectance spectrum of the proposed structure versus changes in dimensional parameters, **(a)** substrate thickness (h_{sub}), **(b)** nanoring thickness (h_r), **(c)** inner radius of nano-rings (R_{in}), and **(d)** outer radius of nano-rings (R_{out}).

best) and the experience of neighboring particles (global best). The iterative process continues until a predefined convergence criterion is met, ensuring that the solution converges toward the global optimum[17].

The PSO algorithm was applied to optimize critical parameters such as substrate thickness, nanoring thickness, and the inner and outer radii of the nano-rings. This approach not only improved the performance metrics of the sensor but also ensured robustness against fabrication tolerances and environmental variations[18]. By integrating the PSO algorithm into the optimization workflow, this study ensures that the proposed plasmonic optical biosensor achieves the highest possible sensitivity and reliability, making it a promising tool for detecting various viruses with precision. The application of PSO in optimizing plasmonic structures has been validated in several recent studies, demonstrating its ability to enhance the performance of nanophotonic devices[19]. Figure 3(a) this section analyzes the impact of substrate thickness on the sensor's reflectance spectrum. The results show that as the substrate thickness increases, the resonance wavelength shifts toward higher values. This phenomenon occurs due to changes in the light-structure interaction and the increased optical path length in the substrate. The optimal substrate thickness for this sensor is determined to be 50 nm, as it maximizes sensitivity and ensures high-quality reflectance spectra. Figure 3(b) Nanoring thickness is another critical parameter in the sensor's design. Increasing the thickness of the nano-rings enhances the intensity of the localized electromagnetic field within the structure, thereby improving the sensor's sensitivity. The results indicate that the optimal nanoring thickness is 150 nm, as it provides the highest reflectance intensity and the narrowest bandwidth. Figure 3(c) the inner radius of the nano-rings directly influences the distribution of the electromagnetic field within the structure. Reducing the inner radius concentrates the electromagnetic field in the central region of the nano-rings, thereby increasing the sensor's sensitivity. The results reveal that the optimal inner radius is 35 nm, as it maximizes the sensor's sensitivity. Figure 3(d) the outer radius of the nano-rings also significantly affects the sensor's performance. Increasing the outer radius enhances the light-structure interaction area, leading to improved sensitivity. The results show that the optimal outer radius is 76 nm, as it provides the highest reflectance intensity and the narrowest bandwidth.

Figure 4(a) examines the effect of temperature variations on the sensor's reflectance spectrum. The results demonstrate that the sensor exhibits stable and reliable performance within the temperature range of 0 to 600 K. Temperature changes have a negligible impact on the resonance peaks and sensitivity of the sensor, indicating high thermal stability of the structure. This stability is attributed to the optimized design of the sensor and the use of materials with stable optical properties at varying temperatures. Such a feature makes the sensor suitable for practical applications in environments with temperature fluctuations. Figure 4(b) analyzes the impact of the angle of incidence on the sensor's reflectance spectrum. The results show that the sensor maintains stable and consistent performance at incident angles of up from 0 to 60 degrees. This feature is due to the symmetric design of the structure and the use of nanostructures capable of absorbing light at various angles. The sensor's stability across different incident angles facilitates its use in real-world conditions and reduces the need for precise angle alignment. Figure 4(c) investigates the effect of light polarization on the sensor's reflectance spectrum. The results indicate that the sensor is polarization-independent, and its performance remains unaffected by changes in the polarization direction. This characteristic is due to the symmetric design and the use of nanostructures capable of absorbing light in all polarization directions. The polarization independence makes the sensor ideal for practical applications in diverse environments, as it eliminates the need for polarization alignment.

The enhancement of the electric field distribution at the resonance wavelength of 1608 nm demonstrates the highly efficient field confinement of the proposed nanostructured sensor, which is demonstrated in Figure. In the XY plane distribution (the top view), as plotted in Fig. 5(a), strong localized electric field is observed inside the nano-rings and in proximity to the nanoholes, indicating the generation of localized surface plasmon resonance (LSPR) and possibly other resonant coupling mechanisms due to the intrinsic geometry of the nanostructure. This high-field confinement is derived from the constructive interference and resonant effect, leading to the periodic and symmetrical distributions of nano-features, which can further focus the optical energy on absolutely small scale. This confinement significantly amplifies the local electromagnetic field, and the structure becomes much more sensitive to changes in the surrounding refractive index. Moreover, Fig. 5(b) of the front view in the XY plane of electric field distribution further demonstrates the results in the XY plane, where a good symmetry characteristic of the electric field is exhibited in the front view in the XZ plane, as shown

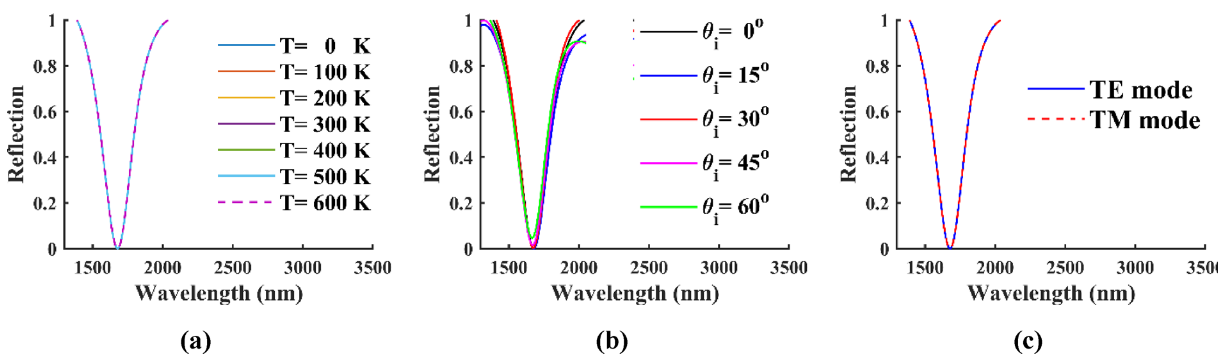

Fig. 4. Investigation of the independence and sustainability of the structure reflection spectrum by examining the effect of **(a)** temperature (T), **(b)** angle of incidence (θ_i), and **(c)** polarization. (TE&TM).

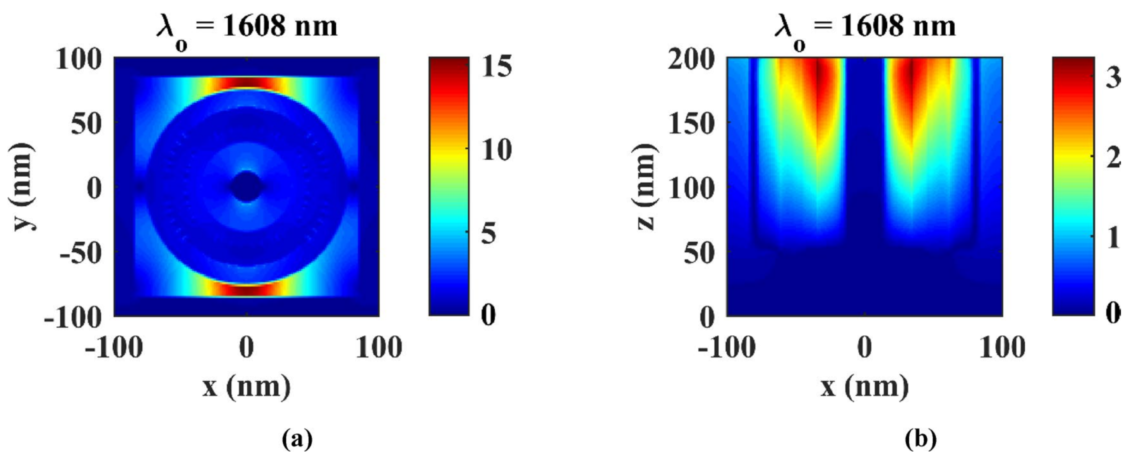

Fig. 5. Representation of the electric field distribution at the resonance wavelength of 1608 nm **(a)** from the top view, i.e., the XY plane, and **(b)** from the front view, i.e., the XZ plane.

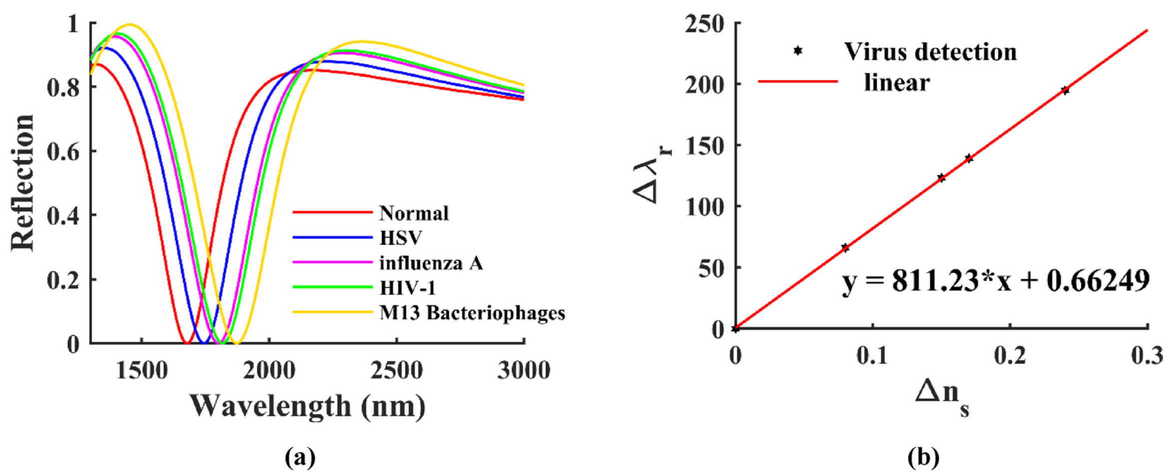

Fig. 6. **(a)** Shift of the sensor reflectance spectrum versus changes in the refractive index of the structure's sensing medium due to the presence of different viruses and **(b)** changes in the resonance wavelength versus changes in the refractive index of the sensing medium due to the presence of different viruses as a curve fit.

in Fig. 5(b). It demonstrates the vertical confinement of the electromagnetic field in the thickness direction of the nanostructures, which also verifies that the incident light is confined both laterally and vertically for the nanostructures. Such 3D field harvesting enhances the overlap between the optical field and the analyte area, to the extent that small changes in the refractive index would cause perceptible shifts of the resonance position. It is this special characteristic that allows the structure to support such highly confined modes and is a consequence of the chosen plasmonic geometry that ensures effective light trapping and long light–matter interaction. These properties combine to give the device a unique ultra-high sensitivity that will make it ideal for use in biochemical sensing and environmental monitoring, among other applications in which nanoscale perturbations in optical properties must be accurately detected.

Figure 6(a) illustrates the shift in the sensor's reflectance spectrum in response to changes in the refractive index of the surrounding medium. The results show that as the refractive index increases, the resonance wavelength shifts toward higher values. This shift occurs due to changes in the light-structure interaction and the increased optical path length in the surrounding medium. The designed sensor is capable of detecting small changes in the refractive index caused by the presence of various viruses, such as HSV, HIV-1, influenza A, and M13 bacteriophages. This feature makes the sensor a powerful tool for biosensing applications.

Figure 6(b) presents the resonance wavelength shift as a function of changes in the refractive index, fitted to a linear curve. The results demonstrate a linear relationship between the refractive index changes and the resonance wavelength shift. This linearity enables the quantitative detection of viruses based on their refractive indices. The slope of this line, representing the sensor's sensitivity, is calculated to be 811 nm.RIU^{-1}. This high sensitivity distinguishes the sensor from previous designs.

Plasmonic sensors, especially those relying on MIM or similar multilayer architectures, have shown high sensitivity, strong local field enhancement, and can be miniaturized to sense small variations of the refractive

References	Sensitivity (nm.RIU^{-1})	FWHM (nm)	FOM (RIU^{-1})
[7]	66	0.9 nm	7.7
[20]	225	–	–
[21]	300	–	–
[6]	313	39.1 nm	4
[22]	430	–	4.4
[23]	750	–	0.43
This work	811	240.04	3.38

Table 3. Comparison of the performance metrics of the four resonance modes of the proposed structure with those from previously published studies.

Sensitivity (nm.RIU^{-1})	FWHM (nm)	FOM (RIU^{-1})	LoD (RIU)	DA (nm^{-1})	SNR	SR (nm)
811	240.04	3.38	0.268	0.004	0.275	217.35

Table 4. All performance metrics of the proposed sensor.

index of the external environment. Utilization of insulator and semiconductor layer between the metal layers can even more facilitate the confinement and propagation of surface plasmon polaritons and consequently will increase the light-matter interaction, leading to better performance of the sensor. These multilayer architectures allow for the fine tuning of resonance conditions, spectral selectivity, and enhancement of local electromagnetic fields, which is of paramount importance for the development of fast, label-free, and ultrasensitive detection. Besides, nanostructures are a good choice for the miniaturization of optical circuits because of their small scale as well as compatibility with nanofabrication processes. Selection of the MISM structure is in line with the present trend in plasmonic sensor design to achieve high sensitivity, tunability, and the possibility of integration for advanced biosensing and chemical detection applications. Also, the integration of MISM technology enables a simple yet effective design and motivates us to further explore its potential. To fabricate these structures, advanced techniques such as electron beam lithography (EBL), focused ion beam lithography (FBL), and nanoimprint lithography are used[11]. Furthermore, microfluidic systems have been integrated for the analysis of liquid medical samples, where changes in resonant frequency due to sample interactions are measured to assess changes in properties[15]. To ensure various designs are manufacturable, optimization should take practical fabrication constraints into account. In particular, minimum feature sizes and alignment tolerances were analyzed to minimize the impact of impossible or challenging-to-build devices. The traditional nanofabrication technique of electron beam lithography (EBL) can reliably be carried out for feature sizes down to ~10 nm, albeit with increasing effort to push below this size because of process constraints. Introducing these constraints in the optimization, end up with device designs that not only achieve high performances but are also realizable through practical fabrication techniques. Table 3 compares the performance metrics of the proposed sensor with some previously published studies, focusing on key parameters such as sensitivity, FWHM, and FOM. These results indicate that the proposed sensor outperforms previous studies regarding sensitivity and FOM. In this study, in addition to analyzing the sensitivity and FOM of the proposed sensor, Other performance metrics, including limit of detection (LoD), detection accuracy (DA), signal-to-noise ratio (SNR), and severity rating (SR), were computed using Eq. 1 to 6 and shown in Table 4.

Conclusion

In this study, a novel plasmonic optical biosensor based on nanoholes and metal-insulator-semiconductor-metal (MISM) nano-rings was designed and analyzed, demonstrating optimal performance in biosensing and medical diagnostics. Simulation results revealed that the proposed design achieves a sensitivity of 811 nm.RIU^{-1} and a figure of merit (FOM) of 3.38 RIU^{-1}, significantly improving compared to previous studies. Additionally, the sensor's limit of detection (LoD) was calculated to be 0.268 RIU, indicating its high precision in detecting small changes in the refractive index of the surrounding environment. The investigation of various parameters, including substrate thickness, inner and outer radii of the nano-rings, and analyte thickness, demonstrated that the structure exhibits high stability against variations in temperature, angle of incidence, and light polarization. Furthermore, incorporating Fano resonance in the sensor's design enhanced its sensitivity and improved the quality of the reflectance spectrum. In summary, the results of this research highlight that the combination of nanoholes and MISM nano-rings can significantly contribute to the development of advanced optical sensors with high sensitivity. However, challenges like achieving high-precision fabrication and minimizing plasmonic losses persist. Future research could focus on optimizing fabrication techniques and conducting experimental tests to evaluate the practical performance of this sensor.

Data availability

The datasets used and/or analyzed during the current study are available from the corresponding author upon reasonable request.

Received: 8 April 2025; Accepted: 16 June 2025
Published online: 01 July 2025

References

1. Tang, Y., Zeng, X. & Liang, J. Surface plasmon resonance: An introduction to a surface spectroscopy technique. *J. Chem. Educ.* **87**, 742–746. https://doi.org/10.1021/ed100186y (2010).
2. Yadav, G. K. & Metya, S. K. Multi fano resonance-based plasmonic MIM nanosensor for label-free virus detection. *IETE J. Res.* **70**, 7597–7606. https://doi.org/10.1080/03772063.2024.2352651 (2024).
3. Huang, W. & Lin, Y. S. Dynamically tunable electric split-ring resonators based on 300 nm gold films on silica for reconfigurable slow-light application. *ACS Appl. Nano Mater.* **6**, 23532–23541. https://doi.org/10.1021/acsanm.3c04908 (2023).
4. Andam, N., Refki, S., Hayashi, S. & Sekkat, Z. Plasmonic mode coupling and thin film sensing in metal–insulator–metal structures. *Sci. Rep.* **11** (1), 15093 (2021).
5. Mostufa, S., Paul, A. K. & Chakrabarti, K. Detection of hemoglobin in blood and urine glucose level samples using a graphene-coated SPR based biosensor. *OSA Contin.* **4** (8), 2164 (2021).
6. Taghipour, A. & Heidarzadeh, H. Design and analysis of highly sensitive LSPR-based metal–insulator–metal nano-discs as a biosensor for fast detection of SARS-CoV-2. In *Photonics* 542. https://www.mdpi.com/2304-6732/9/8/542 (MDPI, 2022).
7. Chorsi, H. T., Zhu, Y. & Zhang, J. X. Patterned plasmonic surfaces—theory, fabrication, and applications in biosensing. *J. Microelectromech. Syst.* **26** (4), 718–739 (2017).
8. Alsalman, O. et al. Design of split ring resonator graphene metasurface sensor for efficient detection of brain tumor. *Plasmonics* **19** (1), 523–532. https://doi.org/10.1007/s11468-023-02002-9 (2024).
9. Taghipour, A. & Heidarzadeh, H. Design and analysis of highly sensitive LSPR-based metal–insulator–metal nano-discs as a biosensor for fast detection of SARS-CoV-2. In *Photonics* 542. https://www.mdpi.com/2304-6732/9/8/542 (MDPI, 2022).
10. Palik, E. D. *Handbook of Optical Constants of Solids*, vol. 3. https://books.google.com/books?hl=en&lr=&id=nxoqxyoHfbIC&oi=fnd&pg=PP1&dq=Palik,+E.D.,+Handbook+of+optical+constants+of+solids.+Vol.+3.+1998:+Academic+press&ots=EH-VJGu2ck&sig=dorKhpqmjsjbc6szE4jkjX8yvqQ (Academic Press, 1998).
11. Zhang, J. et al. Plasmonic metasurfaces with 42.3% transmission efficiency in the visible. *Light: Sci. Appl.* **8** (1), 53 (2019).
12. Zhu, S., Tang, Y., Lin, C., Liu, X. Y. & Lin, Y. Recent advances in patterning natural polymers: From nanofabrication techniques to applications. *Small Methods* **5**, 2001060. https://doi.org/10.1002/smtd.202001060 (2021).
13. Mostufa, S., Paul, A. K. & Chakrabarti, K. Detection of hemoglobin in blood and urine glucose level samples using a graphene-coated SPR based biosensor. *OSA Continuum*. **4** (8), 2164–2176 (2021).
14. Wekalao, J. et al. Detection of proteins in a surface plasmon resonance biosensor based on hybrid metasurface architecture and behaviour prediction using random forest regression. *Plasmonics Dec.* https://doi.org/10.1007/s11468-024-02712-8 (2024).
15. Mauriz, E. Recent progress in plasmonic biosensing schemes for virus detection. *Sensors* **20**, 4745 (2020).
16. Kennedy, J. & Eberhart, R. Particle swarm optimization. In *Proceedings of ICNN'95-International Conference on Neural Networks* 1942–1948. https://ieeexplore.ieee.org/abstract/document/488968/?casa_token=w247mKR24SUAAAAA:eaLkT-fk83wLS429tTPXn0YxoBV-Y45Ct7fBLTkk2yzSaWbU3WElTCjsXOzCK3kofWJiJ50 (IEEE, 1995).
17. Blackwell, T., Kennedy, J. & Poli, R. Particle swarm optimization. *Swarm Intell.* **1** (1), 33–57 (2007).
18. Han, L., Xu, C., Huang, T. & Dang, X. Improved particle swarm optimization algorithm for high performance SPR sensor design. *Appl. Opt.* **60** (6), 1753–1760 (2021).
19. Srivastava, R. et al. On the feasibility of particle swarm optimization method for inverse design of high-performance SPR biosensor, *IEEE Sens. J.* https://ieeexplore.ieee.org/abstract/document/10486829/?casa_token=AyMfSsyshWIAAAAA:qich0DcTWjRdnU-SyKlDVLhAHI_E5qHU8gOFR9f5tw6OfeAuTAHCI5elPHz9KNv63Io7V84 (2024).
20. Vafapour, Z. Polarization-independent perfect optical metamaterial absorber as a glucose sensor in food industry applications. *IEEE Trans. Nanobiosci.* **18** (4), 622–627 (2019).
21. Vafapour, Z. et al. The potential of refractive index nanobiosensing using a multi-band optically tuned perfect light metamaterial absorber. *IEEE Sens. J.* **21** (12), 13786–13793 (2021).
22. Le, K. Q., Ngo, Q. M. & Nguyen, T. K. Nanostructured metal–insulator–metal metamaterials for refractive index biosensing applications: design, fabrication, and characterization. *IEEE J. Sel. Top. Quantum Electron.* **23** (2), 388–393 (2016).
23. Patel, S. K., Surve, J., Parmar, J., Natesan, A. & Katkar, V. Graphene-based metasurface refractive index biosensor for hemoglobin detection: machine learning assisted optimization. *IEEE Trans. Nanobiosci.* **22** (2), 430–437 (2022).

Author contributions

All authors contributed equally to this work.

Declarations

Competing interests

The authors declare no competing interests.

Additional information

Correspondence and requests for materials should be addressed to H.H.

Reprints and permissions information is available at www.nature.com/reprints.